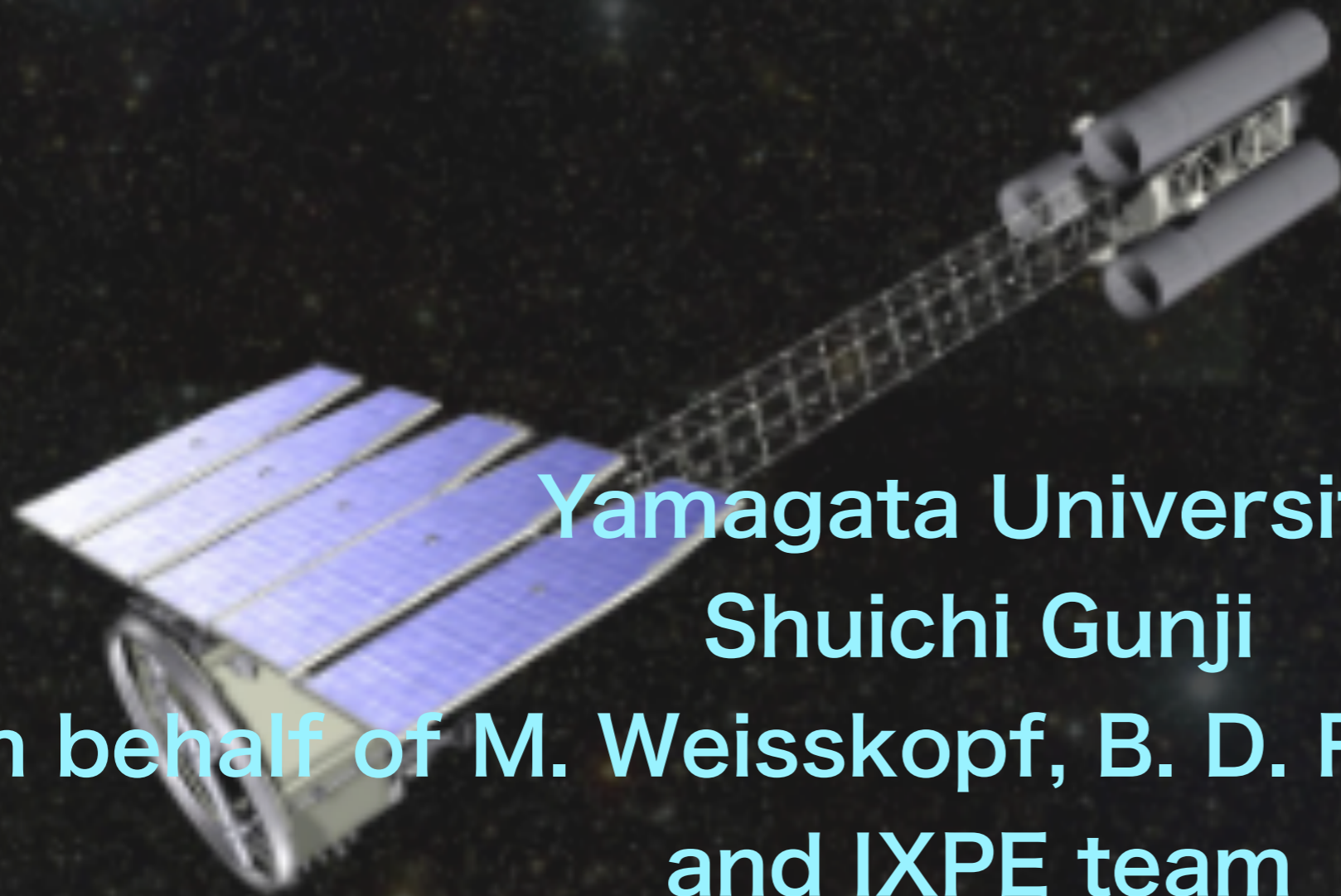


Imaging X-Ray Polarimetry Explorer

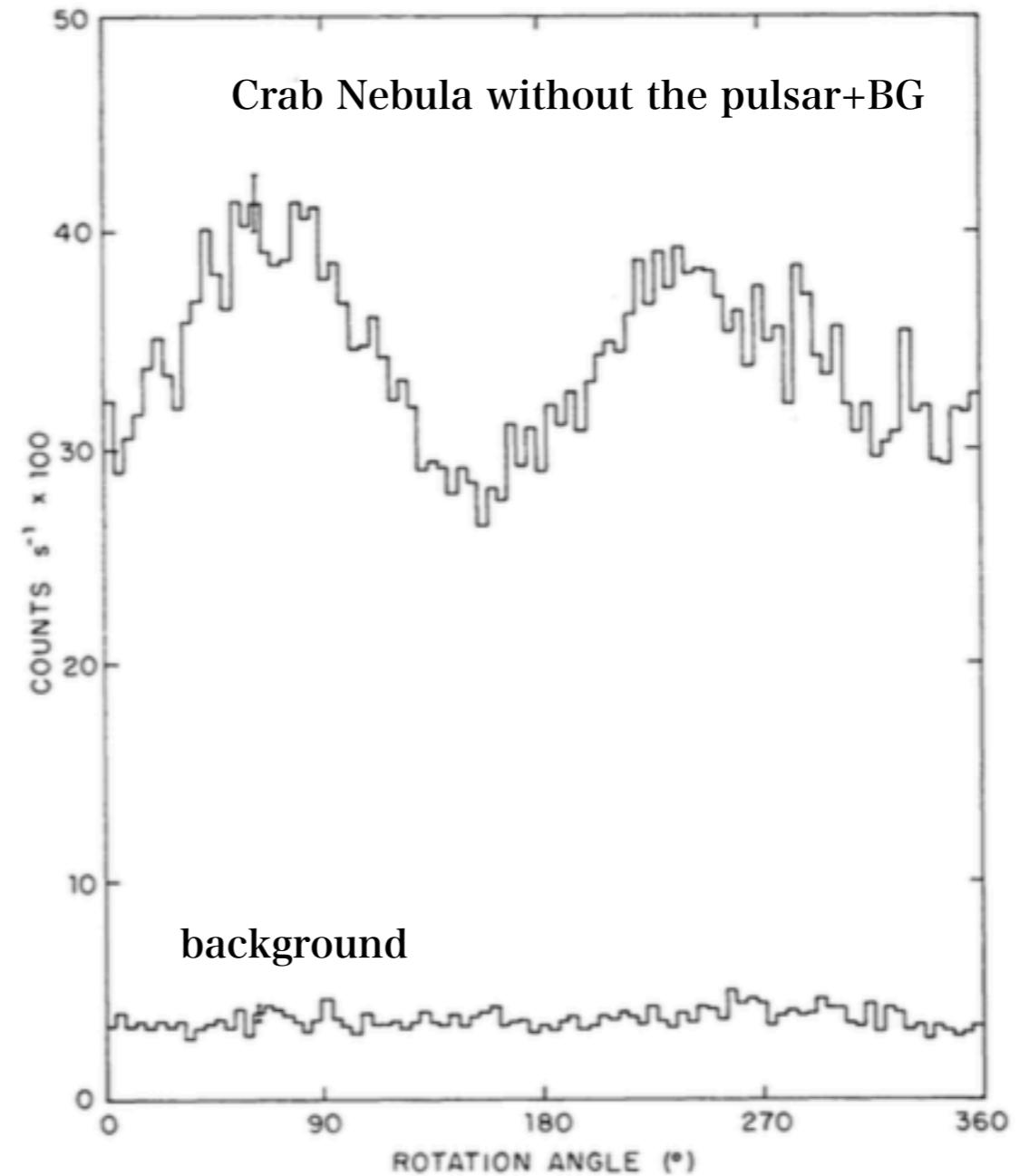
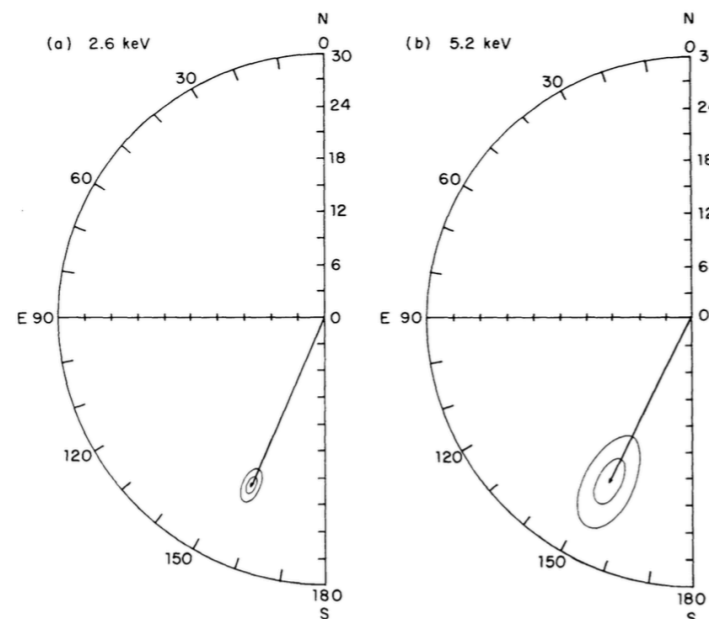
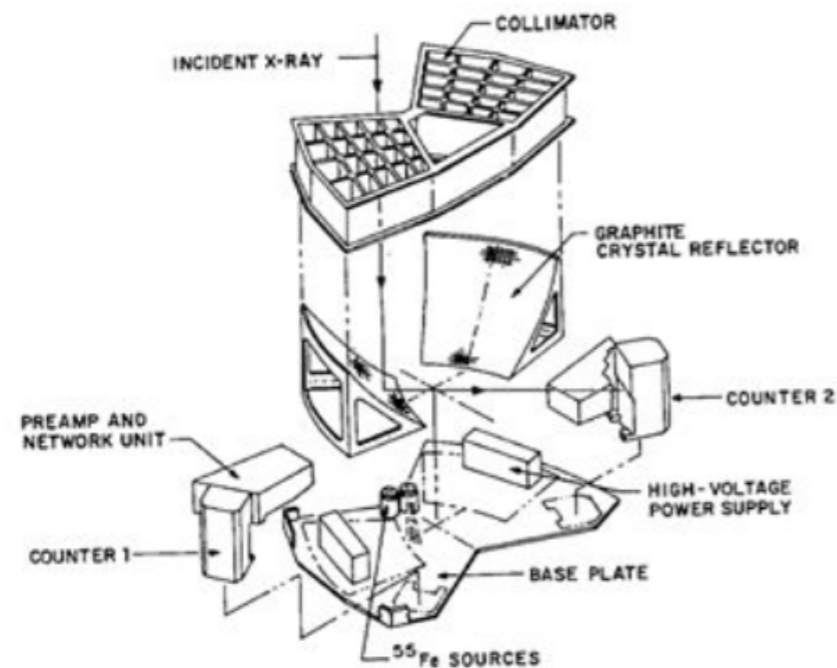


Yamagata University
Shuichi Gunji

On behalf of M. Weisskopf, B. D. Ramsey, S. O'Dell
and IXPE team

1. Introduction

From the measurement of polarization for Crab Nebula by OSO 8, the history of the X-ray polarimetry had started.



Weisskopf et al. Ap.J. 220 (1978)

It also told us the lessons learned to the next step.

Below 10 keV, the expected degree of polarization **will be at most several percents** for black holes, pulsar, AGN, SNR, magnetar, and so on.

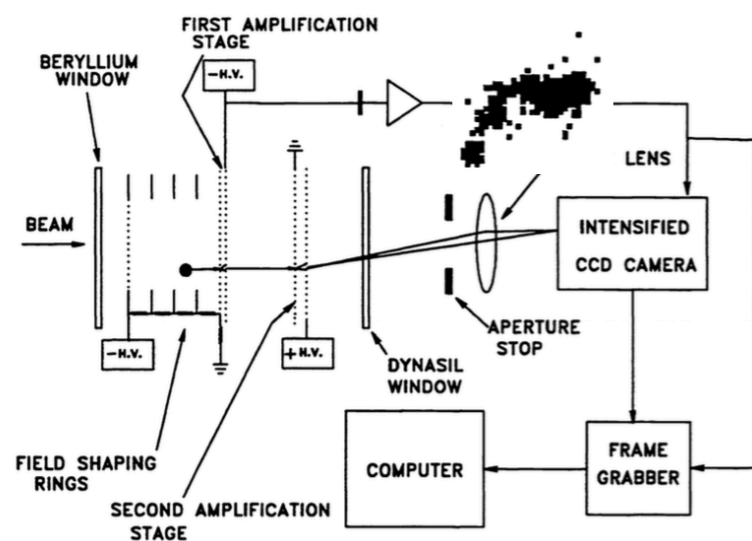


1) We must improve the ratio of the signal to the background.

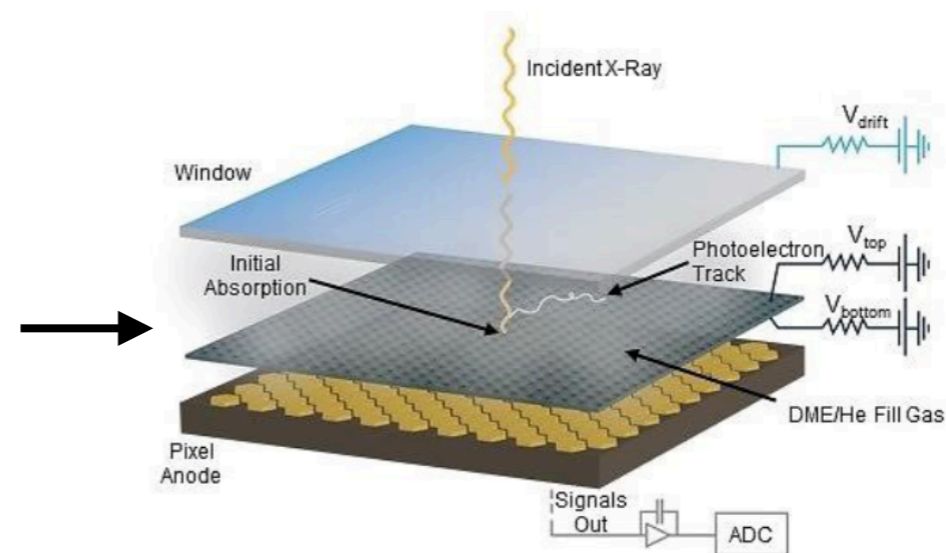
- An x-ray mirror should be used.
- The Bragg polarimeter is sensitive only in certain discrete energies. Required is the polarimeter with wide energy band, better detection efficiency and moderate modulation factor. **The new type of polarimeter is necessary.**

2) The systematic error should be reduced less than ~1%.

- The design of the polarimeter should be symmetrical.
- **The imaging capability can be very useful to investigate the systematic error.**






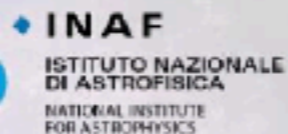







R.A. Austin, T. Minamitani, and
B. D. Ramsey SPIE 2010 (1993)



E.Costa et. al, Nature 411 (2001)

2. IXPE

P.I. : Martin Weisskopf.

| | |
|--|---|
|  PI team, project management, SE and S&MA oversight, mirror module fabrication, X-ray calibration, science operations, and data analysis and archiving |  Polarization-sensitive imaging detector systems |
|  Detector system funding, ground station |  Polarization-sensitive imaging detector systems |
|  Spacecraft, payload structure, payload, observatory I&T |  Polarization-sensitive imaging detector systems |
| |  Mission operations |
| |  UNIVERSITÀ DEGLI STUDI |
| |  Stanford University Scientific theory |
| |  McGill Science Working Group Co-Chair |
| |  Massachusetts Institute of Technology Co-Investigator |

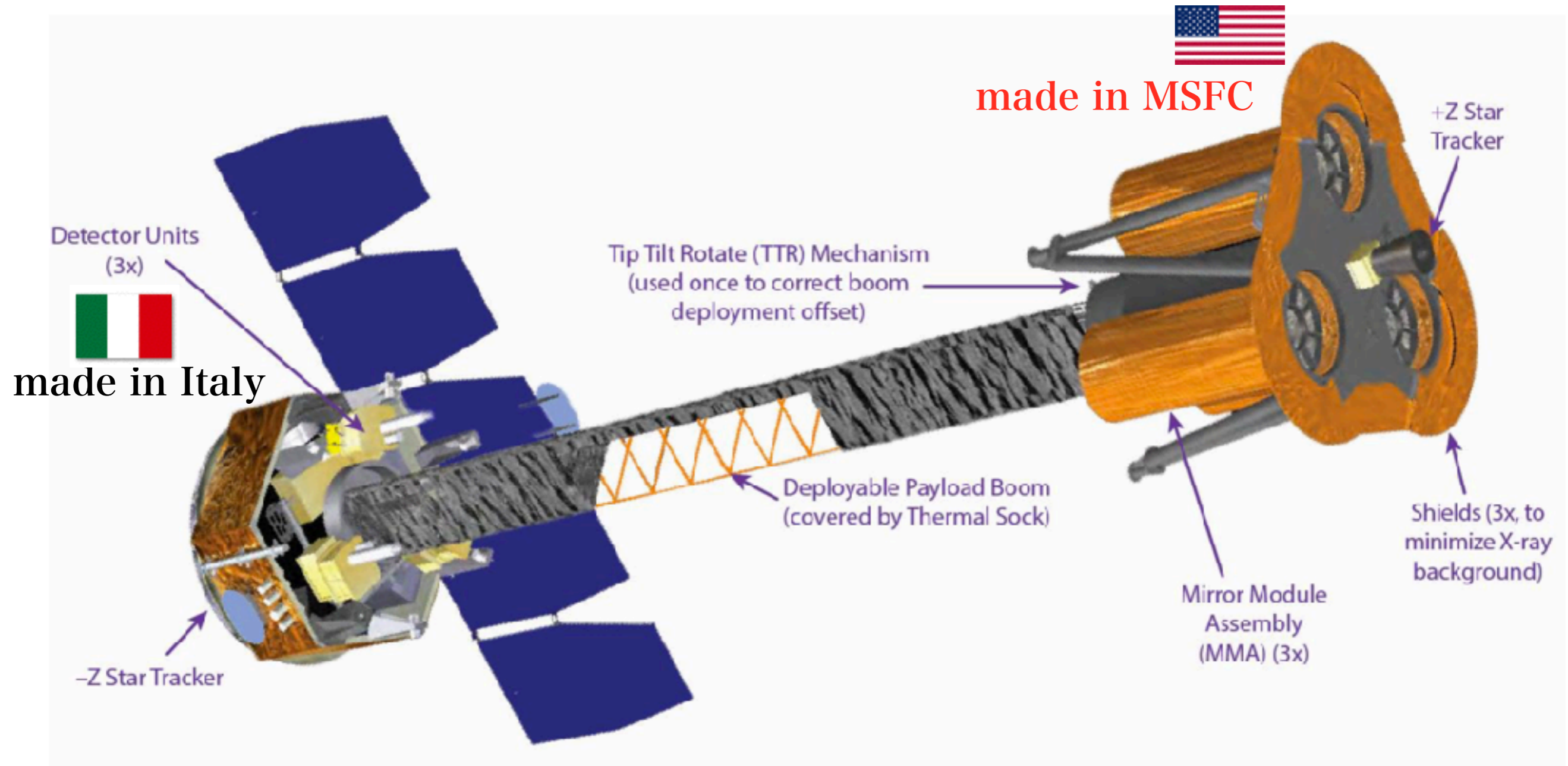
A12567_151



Science Advisory Team

Co-Investigators: Brian D. Ramsey, Paolo Soffitta, Ronaldo Bellazzini, Enrico Costa, Stephen L. O'Dell, Allyn Tennant, Herman Marshall, Fabio Muleri, Jeffery Kolodziejczak, Roger Romani, Giorgio Matt, Victoria Kaspi, Ronald Elsner

Collaborators: L. Baldini, A. Brez, N. Bucciantini, E. Churazov, S. Citrano, E. Del Monte, N. Di Lalla, I. Donnarumma, M. Dovčiak, Y. Evangelista, S. Fabiani, R. Goosmann, S. Gunji, V. Karas, M. Kuss, L. Latronico, A. Manfreda, F. Marin, M. Minuti, N. Omedei, L. Pacciani, G. Pavlov, M. Pesce-Rollins, P.-O. Petrucci, M. Pinchera, J. Poutanen, M. Razzano, A. Rubini, M. Salvati, C. Sgrò, F. Spada, G. Spandre, L. Stella, R. Sunyaev, R. Taverna, R. Turolla, K. Wu, S. Zane, D. Zanetti

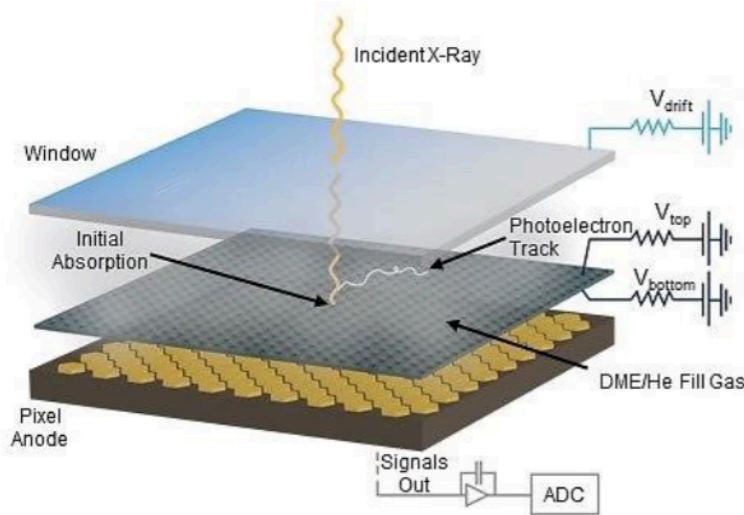


- 1) The X-ray mirror has been developed by NASA/MSFC group including B.D. Ramsey. They has also developed the mirrors such as ART-XC, HEROES, FOXSI, and Micro X.
- 2) The micro pattern gas detector has been developed by Italian group including E. Costa. It has high Technical Readiness Level (TRL).

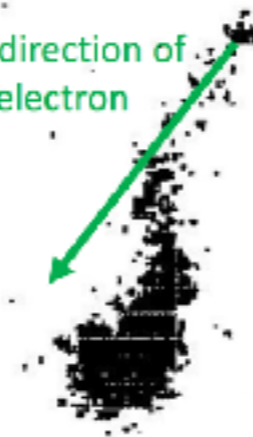
3. The X-ray Mirror Modules

| Parameter | Value |
|------------------------------------|---|
| Number of mirror modules | 3 |
| Number of shells per mirror module | 24 |
| Focal length | 4000 mm |
| Total shell length | 600 mm |
| Range of shell diameters | 162–272 mm |
| Range of shell thicknesses | 0.16–0.26 mm |
| Shell material | Electroformed nickel–cobalt alloy |
| Effective area per mirror module | 230 cm ² (@ 2.3 keV); >240 cm ² (3–6 keV) |
| Angular resolution (HPD) | <u>≤ 25 arcsec</u> |
| Field of view (detector limited) | <u>12.9 arcmin square</u> |

4. The micro pattern gas detector

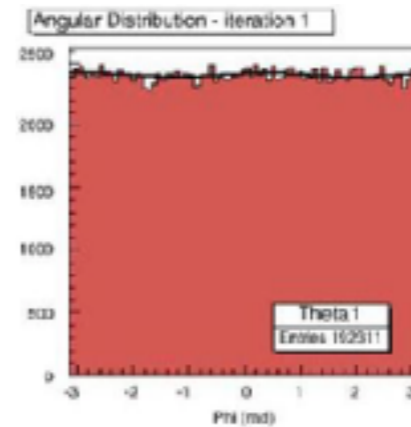


Initial direction of photoelectron



Site of initial ionization and Auger electron cloud

The modulation factor is ~ 50% @ 4keV.



Any systematic effects are very low.

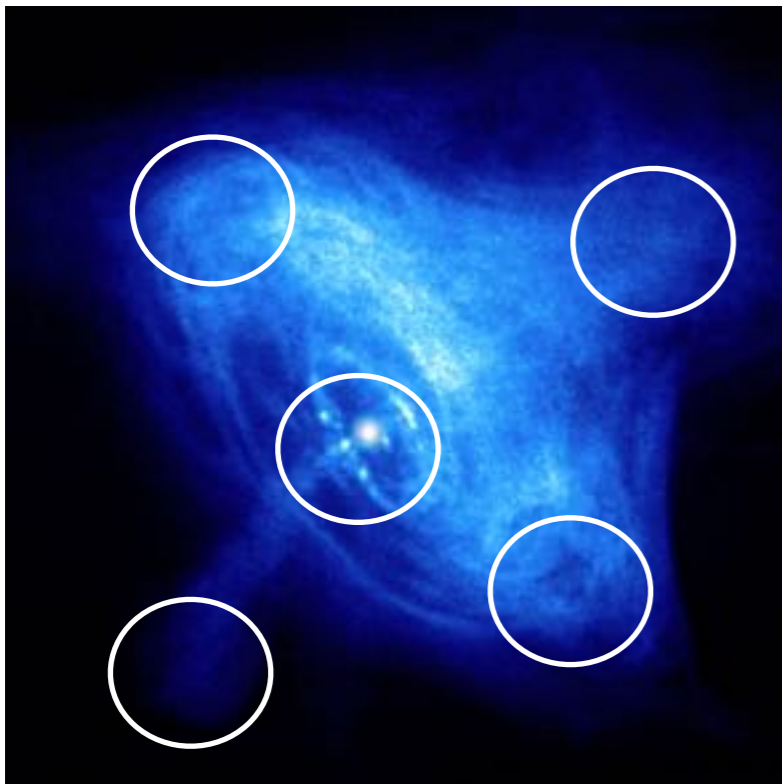
| Parameter | Value |
|-----------------------------------|--|
| Sensitive area | 15 mm × 15 mm |
| Fill gas and composition | He/DME (20/80) @ 1 atm |
| Detector window | 50- μ m thick beryllium |
| Absorption and drift region depth | 10 mm |
| GEM (gas electron multiplier) | copper-plated 50- μ m liquid-crystal polymer |
| GEM hole pitch | 50 μ m triangular lattice |
| Number ASIC readout pixels | 300 × 352 |
| ASIC pixelated anode | Hexagonal @ 50- μ m pitch |
| Spatial resolution (FWHM) | $\leq 123 \mu\text{m}$ (6.4 arcsec) @ 2 keV |
| Energy resolution (FWHM) | 0.54 keV @ 2 keV ($\propto \sqrt{E}$) |

5. Physics

We will observe about 50 stellar objects. For the observations of stellar objects such as PWN, SNR, and AGN, the imaging capability is very useful.

This is a part of the full list and preliminary.

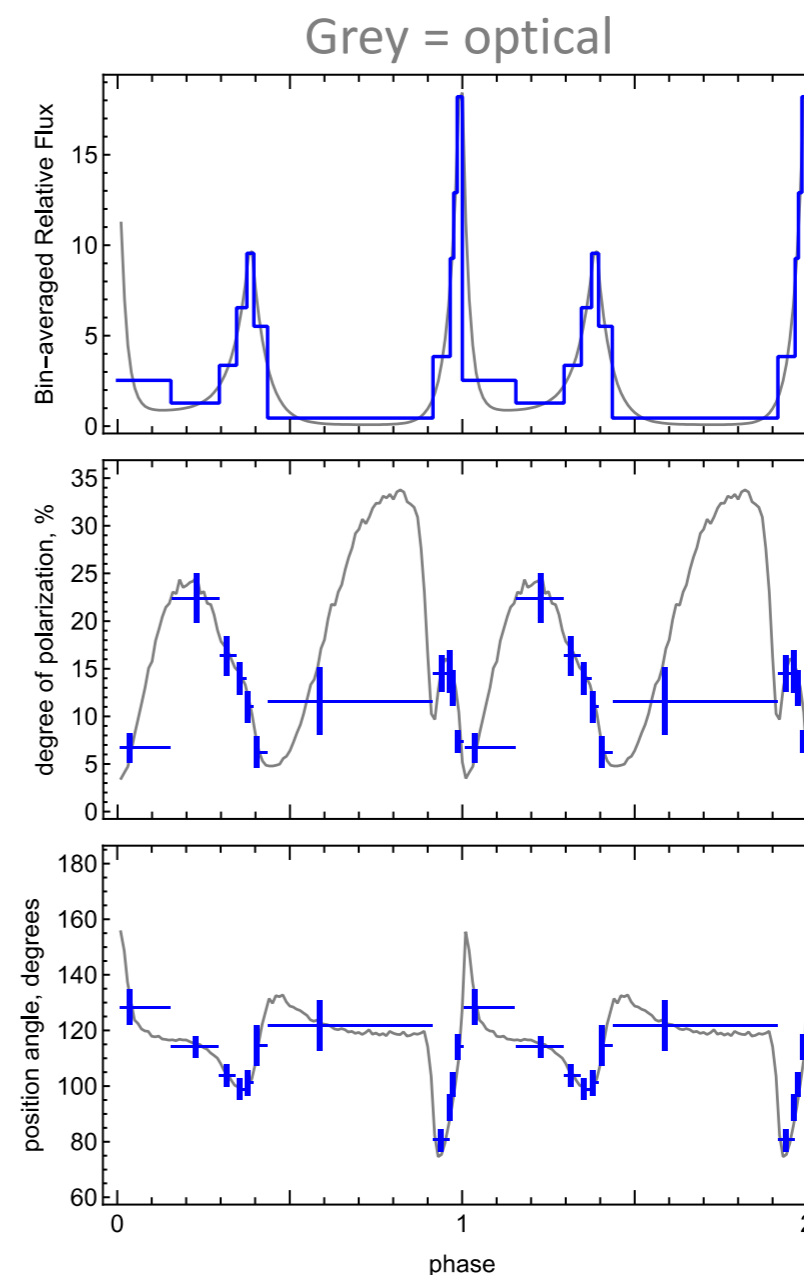
The Crab Nebula and the angular resolution



| Source name | F_{2-3} 10 ⁻¹¹ cgs | MDP ₉₉ % | Δt day | Uncertainty σ_{II} and σ_{ψ} for representative polarization measurements for indicated number of energy \times time or pulse phase \times spatial bins |
|---|------------------------------------|------------------------|-------------------|---|
| Active Galactic Nuclei (AGN) | | | | |
| Gen A radio galaxy | 33.5 | 0.7 | 10.9 | Core (4 bins) $II \pm 0.5\%$, $\psi \pm 2.8^\circ$ (if $II \approx 5\%$) & Jet (4 bins) $II \pm 1.5\%$, $\psi \pm 4.2^\circ$ (if $II \approx 10\%$) |
| Mkn 421 blazar | 27.2 | 2.0 | 1.8 | (3 bins) $II \pm 1.1\%$, $\psi \pm 3.3^\circ$ (if $II \approx 10\%$) |
| Galactic Center | | | | |
| Sgr B2 | 0.30 | 7.5 | 11.6 | (3 bins) $II \pm 4.3\%$, $\psi \pm 2.5^\circ$ (if $II \approx 50\%$), test hypothesis of Sgr A* reflection |
| Microquasars | | | | |
| GRS 1915+105 | 1300. | 0.25 | 2.3 | (4 bins) $II \pm 0.2\%$, $\psi \pm 1.0^\circ$ (if $II \approx 5\%$), with energy, measure black-hole spin |
| Cyg X-3 average | 580. | 0.4 | 2.8 | (4 bins) $II \pm 0.3\%$, $\psi \pm 1.5^\circ$ (if $II \approx 5\%$); MDP = 0.7% in low state |
| Cyg X-1 average | 1000. | 0.4 | 0.7 | (4 bins) $II \pm 0.3\%$, $\psi \pm 1.5^\circ$ (if $II \approx 5\%$); MDP = 0.6% in low state |
| Pulsar-Wind Nebulae (PWNe) + Pulsars (PSR) | | | | |
| Crab PWNe + pulsar | 1950. | 0.24 | 1.8 | PWNe (25 bins) $II \pm 0.4\%$, $\psi \pm 0.6^\circ$ (if $II \approx 20\%$), image magnetic structure Pulsar (9 bins) $II \pm 2.6\%$, $\psi \pm 3.7^\circ$ (if $II \approx 20\%$), 34-ms pulse period, PWNe subtracted |
| Vela PWNe + pulsar | 5.2 | 1.8 | 11.7 | PWNe (18 bins) $II \pm 2.6\%$, $\psi \pm 3.7^\circ$ (if $II \approx 20\%$), image magnetic structure Pulsar (2 bins) MDP = 19.9%, 89-ms pulse period, PWNe subtracted |
| MSH 15-52 + B1509-58 | 7.2 | 1.5 | 12.3 | PWNe (18 bins) $II \pm 2.6\%$, $\psi \pm 3.7^\circ$ (if $II \approx 20\%$), image magnetic structure Pulsar (9 bins) $II \pm 3.1\%$, $\psi \pm 4.4^\circ$ (if $II \approx 20\%$), 151-ms pulse period, PWNe subtracted |
| Supernova Remnants (SNR) | | | | |
| Cas A | 116.0 | 0.35 | 11.6 | (48 bins) $II \pm 0.8\%$, $\psi \pm 4.6^\circ$ (if $II \approx 5\%$), image magnetic structure |
| Magnetars | | | | |
| 4U 0142+61 | 5.9 | 2.0 | 5.4 | (9 bins) $II \pm 2.0\%$, $\psi \pm 1.1^\circ$ (if $II \approx 50\%$), 8.7-s pulse period, test vacuum birefringence |
| Classical Accreting X-ray Pulsars (High-B X-ray Binaries) | | | | |
| Cen X-3 | 341. | 0.5 | 2.6 | (27 bins) $II \pm 0.9\%$, $\psi \pm 1.2^\circ$ (if $II \approx 20\%$), 4.84-s pulse period |
| 4U 0900-40 | 574. | 0.5 | 1.5 | (27 bins) $II \pm 0.9\%$, $\psi \pm 1.2^\circ$ (if $II \approx 20\%$), 283-s pulse period |
| Accreting Millisecond X-ray Pulsars & other Low-B X-ray Binaries | | | | |
| Sco X-1 *0.1 transmission | 2250. | 0.4 | 0.34 | (5 bins) $II \pm 0.3\%$, $\psi \pm 1.7^\circ$ (if $II \approx 5\%$), with bright-source attenuating filter |
| Cyg X-2 | 987. | 0.4 | 1.1 | (5 bins) $II \pm 0.3\%$, $\psi \pm 1.7^\circ$ (if $II \approx 5\%$) |

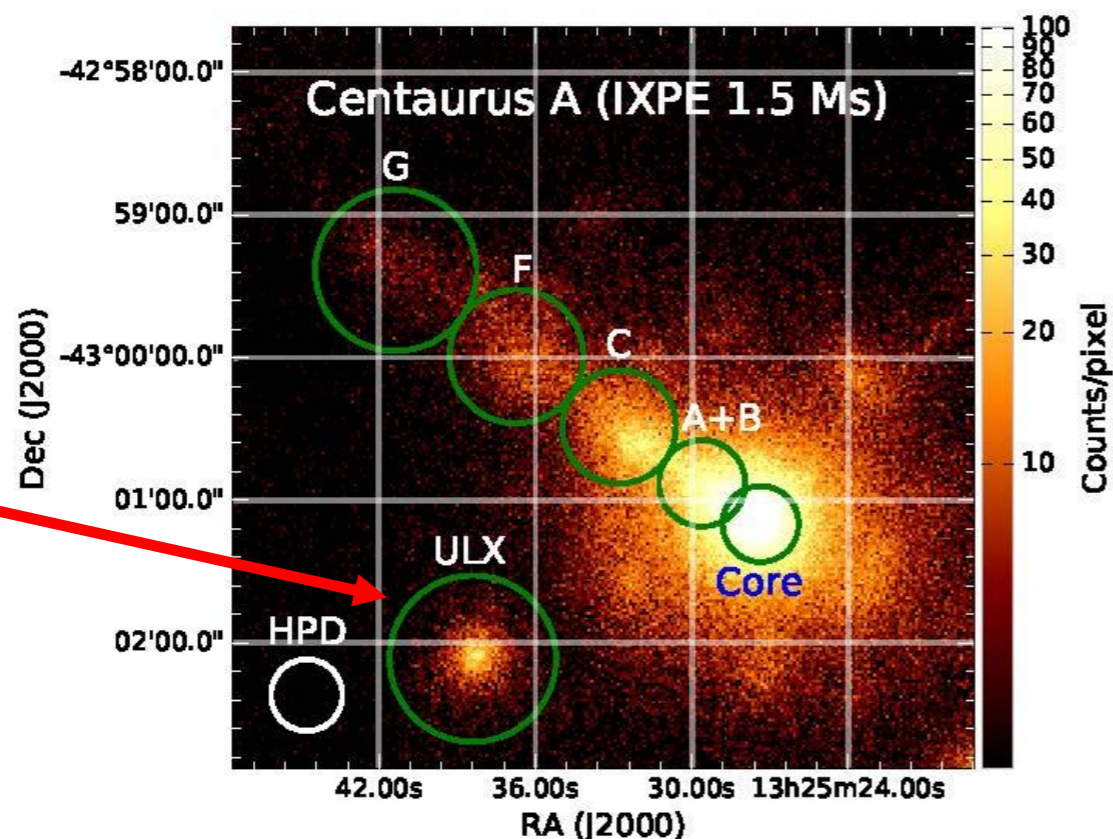
PROBE EMITTING REGIONS OF PULSARS THROUGH PHASE-RESOLVED POLARIMETRY: CRAB PULSAR

- **Emission geometry and processes are unsettled**
 - Competing models predict differing polarization behavior with pulse phase
- **X-rays provide cleaner probe of geometry**
 - Absorption likely more prevalent in visible band
 - Radiation process entirely different in radio band
 - Recently discovered no pulse phase-dependent variation in polarization degree and position angle @ 1.4 GHz
- **140-ks observation gives ample statistics to track polarization degree and position angle**



IXPE IMAGING ALSO AVOIDS CONFUSION AND PROVIDES SERENDIPITOUS BENEFITS

- **Active galaxies are powered by supermassive BHs with jets**
 - Radio polarization implies the magnetic field is aligned with jet
 - Different models for electron acceleration predict different dependence in X-rays
- **Imaging Cen A allows isolating other sources in the field**
 - Two Ultra Luminous X-ray sources (one to SW on detector but not visible in 6-arcmin-square displayed region)



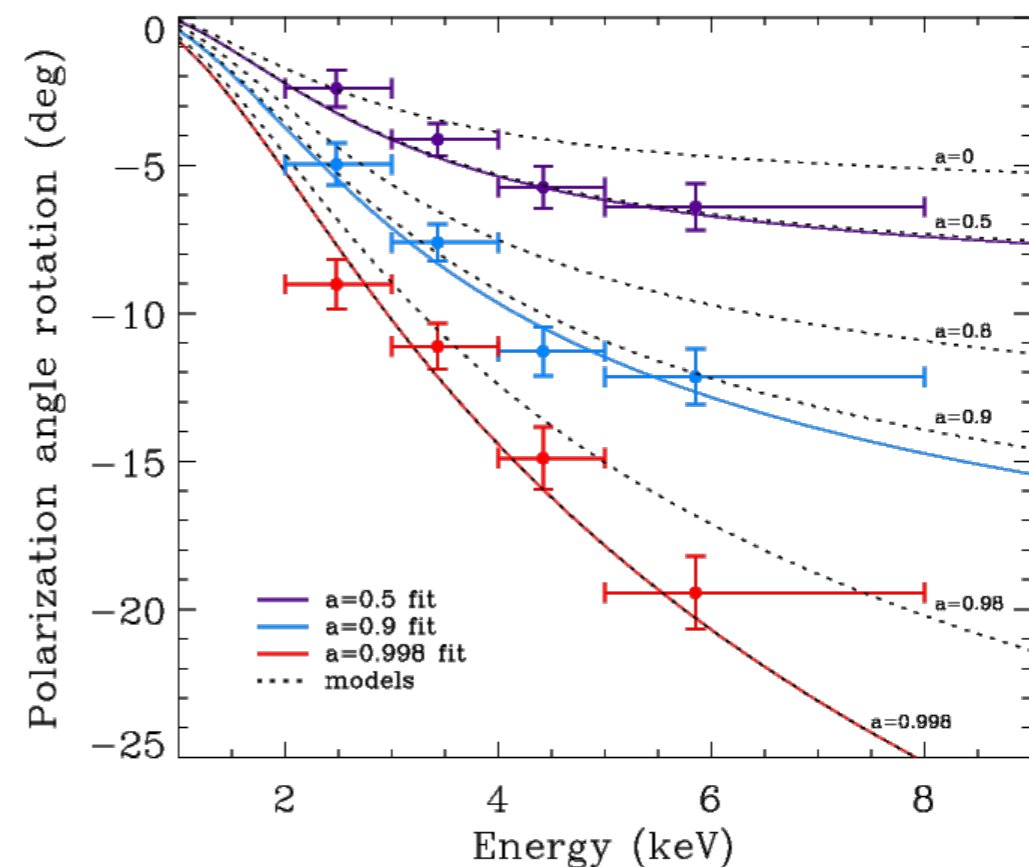
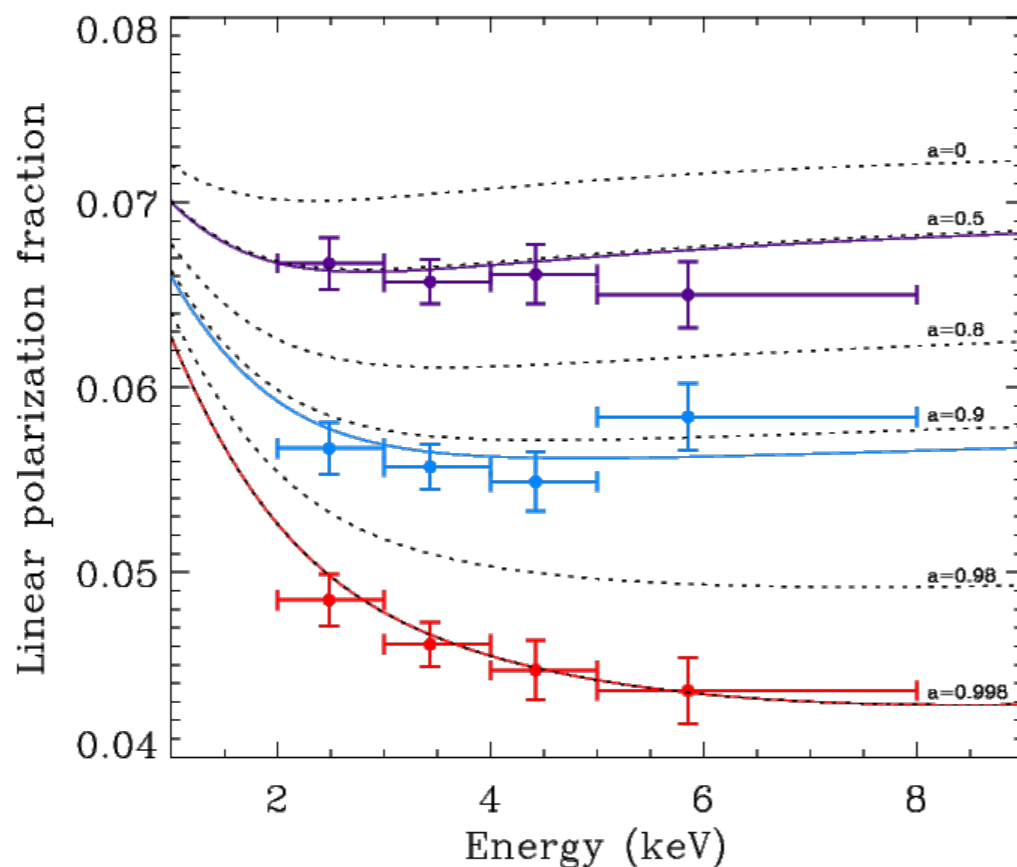
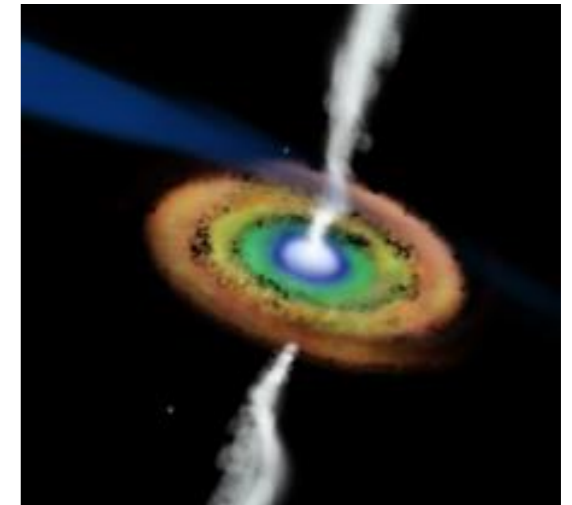
| Region | MDP ₉₉ |
|----------|-------------------|
| Core | <7.0% |
| Jet | 10.9% |
| Knot A+B | 17.6% |
| Knot C | 16.5% |
| Knot F | 23.5% |
| Knot G | 30.9% |
| ULX | 14.8% |

Includes effects of dilution by unpolarized diffuse emission

MEASURE BLACK-HOLE SPIN FROM POLARIZATION

ROTATION IN TWISTED SPACE-TIME: GRS1915+105

- **For a micro-quasar in an accretion-dominated state**
 - Scattering polarizes the thermal disk emission
 - Polarization rotation is greatest for emission from inner disk
 - Inner disk is hotter, producing higher energy X-rays
 - Priors on disk orientation constrain GRS1915+105 model
 - $a = 0.50 \pm 0.04$; 0.900 ± 0.008 ; 0.99800 ± 0.00003 (200-ks observation)



6. Summary

- 1) Since the measurement of polarization for Crab Nebula by OSO-8, about forty years have passed. But the time has come to advance the X-ray polarimetry to the next step. It is Imaging X-ray Polarimetry Explorer.
- 2) The IXPE is international collaboration including NASA/MSFC and Italian team. The main instruments are three X-ray mirrors and micro pattern gas detectors.
NASA/MSFC and Italian group have much heritage for the development.
- 3) The energy range is from 2 keV to 8 keV.
The modulation factor is 50 % @ 4 keV.
The angular resolution is 25'' and the field of view is ~ 13' squares.
- 4) Both diffuse sources and point-like sources are the targets.
In Nov. 2020, it will be launched by Pegasus and their observations of the polarization will be carried out for two years.

The new history of the X-ray polarimetry will be made.